

## Inducing critical phenomena in spin chains through sparse alternating fields

M. Cerezo,<sup>1</sup> R. Rossignoli,<sup>1,2</sup> N. Canosa,<sup>1</sup> and C. A. Lamas<sup>1</sup>

<sup>1</sup>*Instituto de Física de La Plata, CONICET, and Departamento de Física, Universidad Nacional de La Plata, C.C. 67, La Plata 1900, Argentina*

<sup>2</sup>*Comisión de Investigaciones Científicas de la Provincia de Buenos Aires (CIC), La Plata 1900, Argentina*

 (Received 26 August 2018; revised manuscript received 25 November 2018; published 9 January 2019)

We analyze the phase diagram of the exact ground state (GS) of spin- $s$  chains with ferromagnetic XXZ couplings under  $n$ -alternating field configurations, i.e., sparse alternating fields having nodes at  $n - 1$  contiguous sites. It is shown that such systems can exhibit a nontrivial magnetic behavior, which can differ significantly from that of the standard ( $n = 1$ ) alternating case and enable mechanisms for controlling their magnetic and entanglement properties. The boundary in field space of the fully aligned phase can be determined analytically  $\forall n$ , and shows that it becomes reachable only above a threshold value of the coupling anisotropy  $J_z/J$ , which depends on  $n$  but is independent of the system size. Below this value, the maximum attainable magnetization becomes much smaller. We then show that the GS can exhibit significant magnetization plateaus, persistent for large systems, at which the magnetization per site  $m$  obeys the quantization rule  $2n(s - m) = \text{integer}$ , consistent with the Oshikawa, Yamanaka, and Affleck criterion. We also identify the emergence of field-induced spin polymerization, which explains the presence of such plateaus. Entanglement and field-induced frustration effects are also analyzed.

DOI: [10.1103/PhysRevB.99.014409](https://doi.org/10.1103/PhysRevB.99.014409)

### I. INTRODUCTION

One of the distinct hallmarks of cooperative behavior in interacting many-body quantum systems are the critical properties and phase transitions that arise when some control parameter is varied [1–5]. In the last decades, entanglement theory has unveiled new properties of these transitions, providing a deep understanding [6–13]. In this scenario, the emergence of notable phenomena such as frustration [14–17] and magnetization plateaus [18–23] is typically associated with antiferromagnetic systems with competing interactions [24,25] and nontrivial geometries [26]. However, much less is known of the critical properties that could be induced even in simple systems through general nonuniform magnetic fields or couplings. Most investigations on nonuniform fields were focused so far on the alternating or “staggered” case [27–35]. Nonetheless, recent studies with more general nonuniform fields [35,36] have shown that interesting and significant phenomena can emerge, particularly with sparse field configurations [36].

Interacting spin systems provide an adequate framework for studying such nontrivial phenomena. Moreover, the possibility of simulating spin systems with tunable couplings and fields is becoming increasingly feasible due to the recent remarkable advances in quantum control technologies [37–39]. In particular, the paradigmatic XXZ model [1,40–49] can emerge as effective Hamiltonian in different systems [50–62]. For instance, it can be achieved in terms of superconducting charge qubits (SCQ) coupled with a SQUID (superconducting quantum interference device) [50–52]. In SCQ setups, the local field parameters can be controlled by means of a gate voltage applied to each SCQ box and an external magnetic flux is used to modulate the Josephson coupling energy [50].

Other examples comprise trapped ions [38,53–55], cold atoms in optical lattices [37,56–58], photon-coupled microcavities [59], quantum dots [60], etc. The XXZ model has also been employed for implementing quantum information protocols [37–39,60,63,64].

Here, we will show that the application of sparse periodic alternating fields in a ferromagnetic XXZ system of arbitrary spin results in atypical ground-state (GS) phase diagrams, which display nontrivial magnetization plateaus and entanglement properties. In the first place, the boundary in field space of the fully aligned phase, which determines the onset of GS entanglement, can be determined analytically and implies a threshold value of the coupling anisotropy, below which the maximum attainable magnetization becomes much smaller. Such boundary is independent of the system size. It is then shown that such sparse fields can induce other nontrivial magnetization plateaus, persistent for large sizes, as verified through density matrix renormalization group (DMRG) [65–67] calculations. These plateaus are shown to satisfy the well-known Oshikawa, Yamanaka, and Affleck (OYA) criterion [23], which can be here explained simply through field-induced polymers with definite magnetization. We also analyze other aspects such as field-induced frustration, single-spin magnetization, and pairwise entanglement, whose results support the polymerization-based picture.

The model and the  $n$ -alternating field configuration are described in Sec. II, with the boundary of the fully aligned phase and the conditions under which it can be reached discussed in Sec. II A. GS magnetization diagrams are then discussed in Sec. II B, while pairwise entanglement in Sec. II C. The Appendices contain the derivation of analytic expressions for the previous boundary and for entanglement measures at the boundary, and the exact analytic solution of the limit

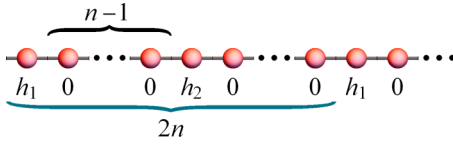


FIG. 1. Schematic representation of a spin chain with an  $n$ -alternating field configuration [Eq. (3)]. The number of intermediate sites with no field is  $n - 1$ . The period is  $2n$ .

case of an XX chain under the present field configurations. Conclusions are drawn in Sec. III.

## II. SPARSE ALTERNATING FIELD CONFIGURATIONS

We consider a cyclic chain of  $N$  spins  $s$  interacting through first-neighbor XXZ couplings in a nonuniform magnetic field along the  $z$  axis. The Hamiltonian reads as

$$H = - \sum_{i=1}^N [h^i S_i^z + J(S_i^x S_{i+1}^x + S_i^y S_{i+1}^y) + J_z S_i^z S_{i+1}^z], \quad (1)$$

where  $h^i$ ,  $S_i^\mu$  are the field and spin components at site  $i$  (with  $N + 1 \equiv 1$ ) and  $J$ ,  $J_z$  the coupling strengths. As  $[H, S^z] = 0$ , with  $S^z = \sum_j S_j^z$  the total spin along the  $z$  axis, its eigenstates can be characterized by the total magnetization  $M = S_z$  ( $-Ns \leq M \leq Ns$ ). We will set  $J > 0$ , as the spectrum and entanglement properties of  $H$  are the same for  $\pm J$  [68]. They are also identical for  $(\{h^j\}, M)$  and  $(\{-h^j\}, -M)$  [69]. It is as well convenient to use the scaled coupling strengths

$$j_z = 2sJ_z, \quad j = 2sJ \quad (2)$$

as critical fields and couplings will depend just on  $j_z$  and  $j$  for different values of  $s$  (see below).

We will here examine the  $n$ -alternating field configuration, depicted in Fig. 1, defined by

$$h^i = \begin{cases} h_1, & i = 1, 2n+1, 4n+1, \dots \\ h_2, & i = n+1, 3n+1, 5n+1, \dots \\ 0, & \text{otherwise} \end{cases} \quad (3)$$

which generalizes the standard alternating (A) case  $(h_1, h_2, h_1, h_2, \dots)$ , recovered for  $n = 1$ . For  $n = 2$  we obtain the “next-alternating” (NA) case  $(h_1, 0, h_2, 0, \dots)$ , while for  $n = 3$  the “next-next-alternating” (NNA) case  $(h_1, 0, 0, h_2, 0, 0, \dots)$ . We set in what follows  $N = 2nK$ , with  $K$  the number of cells with  $2n$  spins.

A motivation for studying the field configurations (3) in the present system is that for  $j_z > j > 0$ , they *all* exhibit, for *any* spin  $s \geq \frac{1}{2}$ , a *multicritical* point in the GS at fields of opposite sign given by [36]

$$h_1 = -h_2 = \pm h_s, \quad h_s = \sqrt{j_z^2 - j^2}, \quad (4)$$

where *all GS magnetization plateaus merge*: At this point, the GS becomes  $2Ns + 1$  degenerate, with the GS’s for each magnetization  $M$  having all the same energy. This point generalizes the Pokrovsky-Talapov (PT) type transition of a spin- $\frac{1}{2}$  chain in an alternating field [27]. Furthermore, at this point there is a whole family of completely separable *factorized* (i.e., product) exact GS’s [36], and the field (4) is then denoted as *factorizing* (or separability) field [36]. It is

independent of the chain size  $K$  and the distance  $n$  between spins with field, depending just on the scaled couplings (2). Here, we will show that the field configurations (3) exhibit other interesting properties in the present system for  $j_z < j$ , being capable of inducing a nontrivial magnetic response.

### A. Border of the aligned phase

A first basic question which arises for  $n \geq 2$  is if such sparse fields are sufficient to induce a completely aligned (and hence completely separable) GS with maximum magnetization  $|M| = Ns$ . In the standard staggered case  $n = 1$ , such phase will always arise for sufficiently strong fields  $h_1, h_2$  of the same sign, for any value of  $j$  or  $j_z$ , but for  $n \geq 2$  the presence of spins with zero field implies that it will not be attainable without the aid of a finite positive value of  $j_z$ , as shown below.

We will prove in fact that for  $n \geq 2$ , the aligned phase with  $|M| = Ns$  is attainable only for

$$j_z > j_z^c(n) = j \cos(\pi/n), \quad n \geq 2 \quad (5)$$

in which case the GS will have  $M = Ns$  if the fields  $(h_1, h_2)$  satisfy  $h_1 + h_2 > 0$  and

$$(h_1 + \beta_n)(h_2 + \beta_n) > \alpha_n^2, \quad (6)$$

with  $h_i > -\beta_n$  such that  $(h_1, h_2)$  lies above the upper branch of the hyperbola, and  $M = -Ns$  if  $h_1 + h_2 < 0$  and

$$(h_1 - \beta_n)(h_2 - \beta_n) > \alpha_n^2, \quad (7)$$

with  $h_i < \beta_n$  such that  $(h_1, h_2)$  lies below the lower branch of a reflected hyperbola. The coefficients  $\alpha_n, \beta_n$  are independent of the size  $K$  and are given by

$$\alpha_n = j \frac{\sinh \gamma}{\sinh n\gamma} = 2h_s \frac{j^n}{(j_z + h_s)^n - (j_z - h_s)^n}, \quad (8)$$

$$\beta_n = j \frac{\sinh \gamma}{\tanh n\gamma} = h_s \frac{(j_z + h_s)^n + (j_z - h_s)^n}{(j_z + h_s)^n - (j_z - h_s)^n}, \quad (9)$$

where  $\cosh \gamma = j_z/j = \Delta$  is the anisotropy and  $h_s = j \sinh \gamma$  the separability field (4), satisfying  $\beta_n^2 = \alpha_n^2 + h_s^2$ . Equations (8) and (9) hold and are real for both  $j_z > j$ , where  $\gamma$  and  $h_s$  are real, and also  $j_z^c(n) < j_z < j$ , where  $\gamma$  and  $h_s$  become imaginary:  $\gamma = i\phi$ , with  $j_z/j = \cos \phi$ ,  $h_s = ij \sin \phi$ , and

$$\alpha_n = j \frac{\sin \phi}{\sin n\phi}, \quad \beta_n = j \frac{\sin \phi}{\tan n\phi} \quad (j_z < j). \quad (10)$$

In the isotropic limit  $j_z \rightarrow j$ ,  $\phi \rightarrow 0$  and  $\alpha_n = \beta_n \rightarrow j/n$ .

*Proof.* The boundary in field space  $(h_1, h_2)$  of the fully aligned phase can be obtained by determining the fields at which the GS undergoes the magnetization transition  $|M| = Ns \rightarrow Ns - 1$ , i.e., where the fully aligned state starts to become unstable against single-spin excitations. The fully aligned states  $|M = \pm Ns\rangle$  are trivial eigenstates of  $H \forall n$  in (3), with energies

$$E_{\pm Ns} = -Ks[\pm(h_1 + h_2) + nj_z], \quad (11)$$

which are independent of  $j$  and degenerate for  $h_1 + h_2 = 0$ . They will be the GS for sufficiently large  $j_z$  and/or strong positive ( $M = Ns$ ) or negative ( $M = -Ns$ ) fields.

On the other hand, the  $|M = Ns - 1\rangle$  eigenstate of lowest energy can be obtained by diagonalizing  $H$  in the invariant

subspace spanned by the  $2n$   $W$ -like [70] states with one spin down (here  $S_i^- = S_i^x - iS_i^y$ ),

$$|W_i\rangle = \frac{1}{\sqrt{2sK}} \sum_{l=0}^{K-1} S_{i+2nl}^- |Ns\rangle, \quad i = 1, \dots, 2n \quad (12)$$

where all sites with the same position  $i$  in the cell have the same weight. These states lead to close and size-independent matrix elements of  $\Delta H = H - E_{Ns}$ :

$$\Delta H |W_i\rangle = (j_z + h^i) |W_i\rangle - \eta_n j (|W_{i+1}\rangle + |W_{i-1}\rangle), \quad (13)$$

where  $h^i = \delta_{i1} h_1 + \delta_{i,n+1} h_2$ ,  $\eta_n = 1 (\frac{1}{2})$  for  $n = 1 (\geq 2)$  and  $|W_0\rangle = |W_{2n}\rangle$ ,  $|W_{2n+1}\rangle = |W_1\rangle$ . A stable  $M = Ns$  GS requires  $\Delta H$  positive definite, entailing positive eigenvalues (excitation energies) of the  $2n \times 2n$  matrix  $\Delta H_n$  of elements

$$(\Delta H_n)_{ij} = \langle W_i | \Delta H | W_j \rangle = \delta_{ij} (j_z + h^i) - \eta_n j \delta_{i,j\pm 1}. \quad (14)$$

This implies the necessary condition

$$\text{Det} [\Delta H_n] > 0. \quad (15)$$

Assuming  $\Delta H$  positive definite for strong positive fields, the  $M = Ns \rightarrow Ns - 1$  transition then occurs at fields  $(h_1, h_2)$  which are the first root of  $\text{Det} [\Delta H_n] = 0$  when approached from the strong positive field limit. From Eq. (14) it is seen that this determinant has the form

$$\text{Det} [\Delta H_n] = a_n h_1 h_2 + b_n (h_1 + h_2) + c_n \quad (16)$$

$$= a_n [(h_1 + \beta_n)(h_2 + \beta_n) - \alpha_n^2], \quad (17)$$

with  $\beta_n = b_n/a_n$ ,  $\alpha_n^2 = \beta_n^2 - c_n/a_n$ , and  $a_n, b_n, c_n$  field independent. Their expressions (8) and (9) are derived in Appendix A, where it is shown that  $a_n \geq 0$  [Eq. (A2)]. Then, positivity of  $\Delta H$  implies fields  $(h_1, h_2)$  satisfying (6), with  $h_i > -\beta_n$ . And stability with respect to the  $M = -Ns$  GS requires  $h_1 + h_2 > 0$  [Eq. (11)]. A similar procedure shows that an aligned GS with  $M = -Ns$  requires fields satisfying (7) with  $h_i < \beta_n$  and  $h_1 + h_2 < 0$ .

As  $j_z/j$  decreases below 1, the denominators in (10) become smaller, *vanishing* for  $\phi \rightarrow \pi/n$  if  $n \geq 2$ , i.e., for  $j_z$  approaching the critical value (5). This implies the *divergence* of  $\alpha_n$  and  $\beta_n$ , and hence of the critical fields, in this limit [note that  $\beta_n < 0$  for  $j_z^c(n) < j_z < j_z^c(2n)$ ]. The fully aligned phase becomes then *unreachable* for  $j_z \leq j_z^c(n)$  ( $\phi \geq \pi/n$ ). This result can also be directly derived from (14): As shown in Appendix A, the lowest eigenvalue  $\lambda_0(n)$  of the matrix  $\Delta H_n$  satisfies

$$\lambda_0(n) < j_z - j \cos(\pi/n), \quad (18)$$

with the upper bound reached for  $h_1, h_2 \rightarrow +\infty$ . Thus, for  $j_z \leq j \cos(\pi/n)$ ,  $\Delta H_n$  has a negative eigenvalue at all finite fields and the aligned state cannot be a GS. It is also verified that at the critical value  $j_z = j \cos(\pi/n)$ ,  $a_n, b_n$ , and  $c_n$  in Eq. (16) *vanish*, i.e.,  $\text{Det} [\Delta H_n] = 0 \forall (h_1, h_2)$  (see Appendix A). ■

The hyperbolas which delimit the aligned phase in Eqs. (6) and (7) also represent *the onset of GS entanglement*, and correspond to an *entanglement transition*: The  $|M = Ns - 1\rangle$  GS will be of the form  $\sum_{i=1}^{2n} w_i |W_i\rangle$ , with  $w_i > 0$  and  $\sum_{i=1}^{2n} w_i^2 = 1$ , which is an entangled state.

Due to the form (12) of the states  $|W_i\rangle$ , pairwise entanglement will reach *full range* in this sector since the ensuing reduced state of two spins,  $\rho_{ij}$ , will depend just on their positions  $i, j$  within the cell *but not on their distance*, i.e., on the number of cells between them. Since  $\rho_{ij}$  is a mixed state, its entanglement can be measured through the entanglement of formation  $E_f(\rho_{ij})$  [71], defined as the convex roof extension of the pure state entanglement entropy. Moreover, as the present  $\rho_{ij}$  can be considered as an effective two-qubit state,  $E_f(\rho_{ij})$  can be determined analytically by means of the concurrence [72]  $C_{ij} = C(\rho_{ij})$ , which is itself an entanglement measure [73], with  $C_{ij} = 1$  (0) for a maximally entangled (separable) mixed state (see Appendix B for details and precise definitions of these quantities). As  $\rho_{ij}$  is independent of the distance between the spins, so is the pairwise concurrence, which is given by (see again Appendix B)

$$C_{ij} = 2|w_i w_j|/K. \quad (19)$$

This value *saturates* the monogamy relations [74,75].

On the other hand, at the mean field level the separable fully aligned states are the trivial symmetry-preserving mean field solutions, and the hyperbolas in Eqs. (6) and (7) represent the onset of the *symmetry-breaking* mean field phase, i.e., of degenerate mean field solutions with  $\langle S_i^\mu \rangle \neq 0$  for  $\mu = x$  or  $y$  (see also Appendix A). For  $j_z \leq j_z^c(n)$ , the aligned solutions are unstable at all fields.

We finally remark that for  $j_z < j_z^c(n)$ , the instability of the aligned state also holds at the single cell level, entailing that a whole interval of magnetizations (at least  $Ns - K + 1 \leq M \leq Ns$ ) also cease to be stable, as will be verified in the next section.

*The first three cases.* Let us now examine the particular cases  $n = 1, 2$ , and 3 in Eq. (3). In the standard staggered case  $n = 1$ , Eqs. (8)–(10) lead to

$$\alpha_1 = j, \quad \beta_1 = j_z, \quad (20)$$

being then verified from (6) and (7) that the aligned phase is reachable  $\forall j, j_z$  for sufficiently strong  $h_1, h_2$ . However, in the NA case  $n = 2$ , they imply

$$\alpha_2 = \frac{j^2}{2j_z}, \quad \beta_2 = j_z - \frac{j^2}{2j_z}, \quad j_z > 0 \quad (21)$$

which *diverge* for  $j_z \rightarrow j_z^c(2) = 0$ . Increasingly stronger fields are here required to reach the aligned phase as  $j_z$  decreases, diverging in the XX limit  $j_z = 0$ . For  $j_z \leq 0$  it becomes unreachable (see also Appendix C).

And in the NNA case  $n = 3$ , Eqs. (8)–(10) lead to

$$\alpha_3 = \frac{j^3}{4j_z^2 - j^2}, \quad \beta_3 = j_z \frac{4j_z^2 - 3j^2}{4j_z^2 - j^2}, \quad j_z > j/2 \quad (22)$$

which *diverge* already for  $j_z \rightarrow j_z^c(3) = j/2$ . The aligned GS cannot be reached for  $j_z \leq j/2$ . The critical fields and couplings of these three cases are depicted in Fig. 2, with the GS magnetization diagrams shown in Fig. 3.

*The parallel critical field.* Equations (6)–(10) also entail that if  $j_z^c(n) < j_z < j$ , full alignment requires application of nonzero fields. For  $h_1 = h_2 = h$ , they imply

$$|h| > h_c^{\parallel}(n) = \alpha_n - \beta_n = j \sin \phi \tan \frac{n\phi}{2}, \quad (23)$$

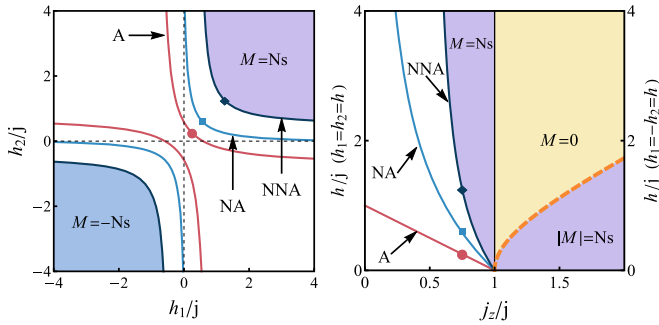


FIG. 2. GS phase diagrams for spin- $s$  XXZ chains in the alternating ( $n = 1$ , A), “next-alternating” ( $n = 2$ , NA), and “next-next-alternating” ( $n = 3$ , NNA) field configurations. Left: the hyperbola branches of Eqs. (6) and (7) delimiting the fully aligned  $M = \pm Ns$  phases at  $j_z/j = 0.75$ . Colored regions indicate GS magnetization  $|M| = Ns$  for all three cases. Right: the threshold (23) of the GS aligned phase for parallel fields  $h_1 = h_2 = h$  and  $j_z < j$ , which diverges for  $j_z \rightarrow 0$  ( $j/2$ ) in the NA (NNA) case, and its upper limit (4) (dashed line) for antiparallel fields  $h_1 = -h_2 = h$  and  $j_z > j$ , common for all  $n$ . Points indicate the thresholds for  $h_1 = h_2$  at  $j_z/j = 0.75$ .

which defines a parallel critical field  $h_c^{\parallel}(n)$ . And if  $h_2 = 0$ , a single field  $|h_1| > -h_s^2/\beta_n = h_c^{\parallel}(2n)$  is sufficient provided  $\beta_n > 0$ , i.e.,  $\phi < \frac{\pi}{2n}$ , which is equivalent to  $j_z > j_z^c(2n)$  ( $h_2 = 0$  in the  $n$ -alternating configuration is equivalent to  $h_2 = h_1$  in the  $2n$ -alternating case).

In contrast, for  $j_z > j$  the GS is fully aligned already at zero field  $\forall n$  and lower magnetizations  $|M|$  arise only for fields of *opposite* sign beyond the factorizing points  $h_1 = -h_2 = \pm h_s$  [36], where *all* magnetization plateaus coalesce, as seen in the bottom panels of Fig. 3. The upper and lower branches of the hyperbolas (6) and (7) intersect precisely at these points  $\forall n$ , providing the border of the aligned phase just beyond these points. Between them, the aligned phases touch at the line  $h_1 + h_2 = 0$ . Note also that for  $j_z > j$  and  $n > 1$ ,  $\alpha_n$  becomes rapidly small for large  $n$  [ $\alpha_n \approx 2h_s(\frac{j}{j_z+h_s})^n$ ] or large  $\frac{j}{j_z}$  [ $\alpha_n \approx j(\frac{j}{2j_z})^{n-1}$ ], implying  $\beta_n \approx h_s$  and hence nonalignment ( $|M| < Ns$ ) just for  $|h_i| \gtrsim h_s$  for  $i = 1, 2$  (and  $h_1 h_2 < 0$ ).

When formally extended to all values of  $j_z$ , the antiparallel (4) and parallel (23) critical fields fully determine  $\alpha_n$  and  $\beta_n$ , and hence the whole border of the aligned phase:

$$\begin{aligned} \alpha_n &= \frac{1}{2}[\pm h_c^{\parallel}(n) - h_s^2/h_c^{\parallel}(n)], \\ \beta_n & \end{aligned} \quad (24)$$

where  $h_c^{\parallel}(n) = -j \sinh \gamma \tanh \frac{n\gamma}{2}$  for  $j_z > j$ . For  $j_z \rightarrow j$  both vanish but  $-h_s^2/2h_c^{\parallel}(n) \rightarrow j/n$ .

### B. Magnetization

A second fundamental question which arises is if magnetization plateaus with  $|M| < Ns$  of *significant width* do also emerge. For large systems, the GS will indeed possess such plateaus (Fig. 4), at which the scaled magnetization  $m = M/(Ns)$  obeys the quantization rule

$$2ns(1 - m) = q, \quad (25)$$

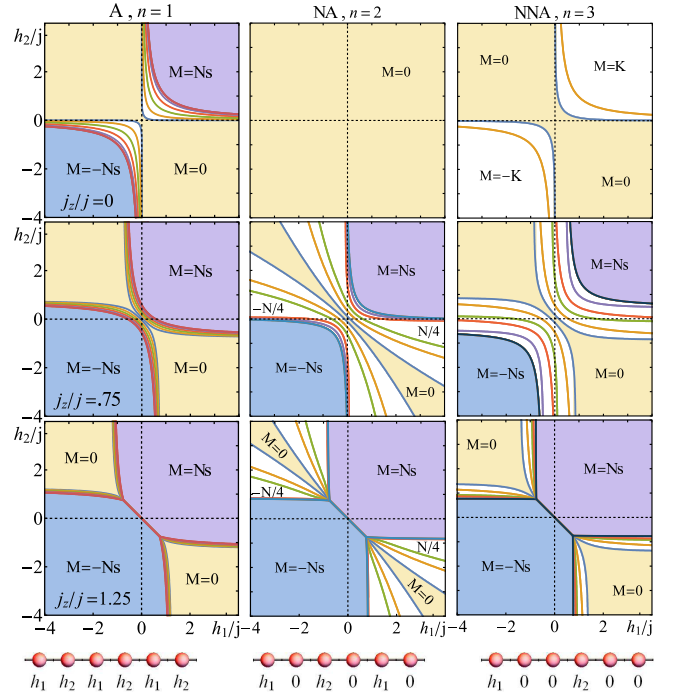


FIG. 3. GS magnetization diagram in the  $(h_1, h_2)$  field plane for an  $N = 12$  spin- $\frac{1}{2}$  XXZ chain in an  $n = 1$  (left),  $n = 2$  (center), and  $n = 3$  (right) field configuration (3), for anisotropies  $j_z/j = 0$  (top),  $0.75$  (center), and  $1.25$  (bottom). Curves separate different magnetizations. For  $j_z = 0$  the GS reaches all magnetizations  $-N/2 \leq M \leq N/2$  in the A case, but remains at  $M = 0 \forall (h_1, h_2)$  in NA, and reaches just the  $M = \pm K = \pm 2$  plateaus in NNA fields. For  $j_z/j = 0.75$ , the three configurations reach all magnetizations, as now  $j_z > j_z^c(n)$ , although the NA case stands out for its wide  $|M| \leq N/4$  sectors. For  $j_z > j$ , magnetizations  $|M| < N/2$  are reached only for fields of opposite sign beyond the factorization points  $h_1 = -h_2 = \pm h_s$ , independent of  $n$ . Bottom row: schematic representation of field configurations.

with  $q$  integer. This result can be readily understood by considering the situation where one of the fields ( $h_1$ ) is sufficiently strong so that the spin chain can be viewed approximately as  $K$  *polymerized subsystems* consisting of  $2n - 1$  spins  $s$  with a field  $h_2$  at the central site (Fig. 1), separated by fully aligned spins. When  $h_2$  is varied, the polymer GS magnetizations  $M_{2n-1}$  will be  $(2n - 1)s - q$  with  $q$  integer, starting from  $q = 0$  when  $j_z > j_z^c(n)$ . Therefore, the total GS magnetization will be  $K\{s + [(2n - 1)s - q]\}$ , entailing then (25) and meaning that *the plateaus in  $m$  reflect essentially the polymer magnetizations*. Due to the periodicity, Eq. (25) is consistent with the OYA criterion [23] (normally used in antiferromagnetic chains in uniform fields). Intermediate magnetizations arise then in the transition regions between these plateaus and imply no definite magnetization at the single cell level.

In Fig. 3 we show representative results for the GS magnetization in a small spin- $\frac{1}{2}$  chain. In the standard alternating case  $n = 1$  (left panels), the GS reaches *all* magnetizations for any anisotropy  $j_z/j$ , with the fully aligned  $|M| = N/2$  sectors separated from the  $M = 0$  plateau by a narrow band containing all intermediate magnetizations. In contrast, in an

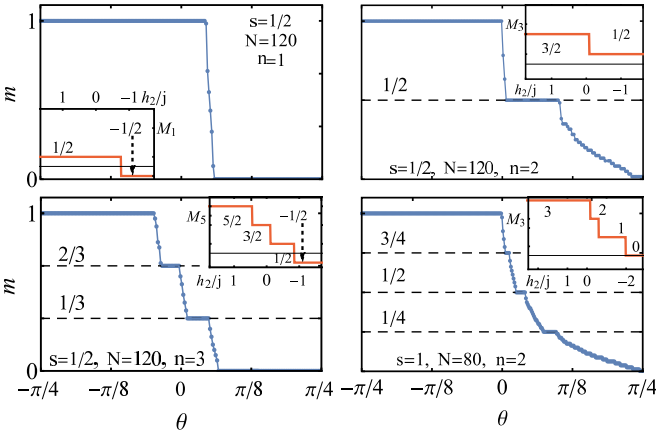


FIG. 4. Scaled GS magnetization  $m = M/(Ns)$  for  $j_z/j = 0.75$  and fields  $(h_1, h_2) = 4j(\cos \theta, -\sin \theta)$ . Results for  $s = \frac{1}{2}$ ,  $N = 120$  spins and  $n = 1, 2, 3$ , and for  $s = 1$ ,  $N = 80$  spins and  $n = 2$ , are depicted. Insets show the polymer magnetizations  $M_{2n-1}$ .

$n = 2$  NA configuration (center), it is first verified that for  $j_z = j_z^c(2) = 0$ , the GS cannot be fully aligned. Moreover, it has strictly  $M = 0$  for all fields, as can be rigorously shown through its Jordan-Wigner fermionization [2] (see Appendix C). For  $j_z > 0$ , this configuration exhibits a noticeable behavior, showing wide  $0 \leq |M| \leq N/4$  sectors in addition to the aligned phases, with the  $|M| = N/4$  plateau persisting for large  $N$  (see below). Finally, in the NNA  $n = 3$  case (right), it is again verified that if  $j_z \leq j_z^c(3) = j/2$ , the GS cannot be fully aligned (top panel), reaching instead a maximum magnetization  $|M| = 2sK = N/6$  for  $j_z = 0$  (and also  $0 < j_z < j/2$  if  $s = \frac{1}{2}$ ). For strong parallel fields, spins with field become aligned while those without form essentially *entangled dimers* with zero magnetization, entailing  $|M| = 2sK$ . When  $j_z > j/2$ , the magnetization diagram becomes similar to that of the  $n = 1$  case, although with a much wider transition sector between the  $M = 0$  and  $|M| = N/2$  plateaus.

Previous results imply that the threshold  $j_z^c(n)$  of the aligned phase is actually a *critical point* below which a whole interval of magnetizations cease to be reachable. This can be understood again from the strong-field limit  $h_1, h_2 \rightarrow \infty$ , where spins with field are fully aligned while those without form essentially isolated chains of  $n - 1$  spins, with effective fields  $sJ_z$  at the end points: For  $n = 2$  and  $j_z \rightarrow 0^+$ , all magnetizations  $M \geq 0$  (and not just  $N/2$  and  $N/2 - 1$ ) of the whole chain become degenerate at strong fields since the  $M_1 = \pm \frac{1}{2}$  states of each of the  $2K$  single spins without field become degenerate, remaining just  $M = 0$  for  $j_z \leq 0$ . Similarly, for  $n = 3$  and  $j_z \rightarrow j/2$ , all chain magnetizations  $M \geq 2sK = N/6$  become degenerate at strong fields since each pair without field may have magnetizations  $M_2 = 1$  or  $0$ , degenerate precisely at  $j_z = j/2$ .

In Fig. 4 we show the GS scaled magnetization for a chain of  $N = 120$  spins  $\frac{1}{2}$ , obtained with density matrix renormalization group (DMRG) [65–67,76]. In the  $n = 1$  case, the transition region from  $M = 0 \rightarrow N/2$  is again quite narrow (top left), in agreement with (25), since here the “polymer” formed for large  $h_1$  consists of just one spin  $s$ , whose lower

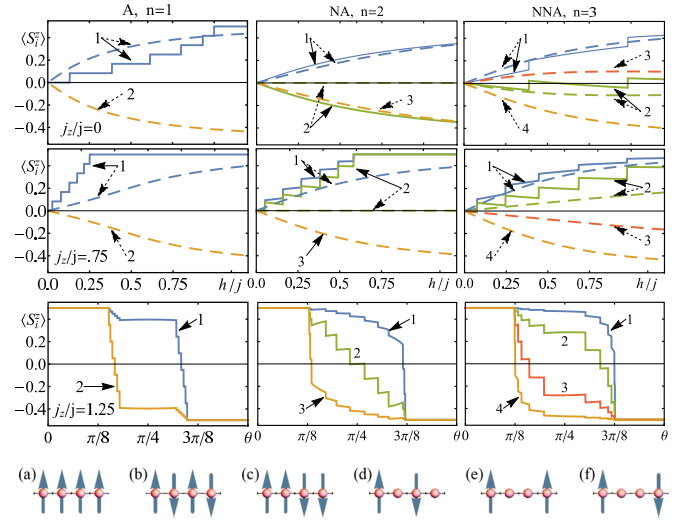


FIG. 5. Top: individual magnetizations  $\langle S_i^z \rangle$  of the first four spins in the same chains of Fig. 3. In the first and second rows, solid lines depict magnetizations for parallel fields  $h_1 = h_2 = h$ , and dashed lines for antiparallel fields  $h_1 = -h_2 = h$ , while in the third row fields are selected as  $(h_1, h_2) = 2j(\cos \theta, -\sin \theta)$ , with  $\theta \in (0, \pi/2)$ . The steps in  $\langle S_i^z \rangle$  reflect those of the total magnetization  $M$ . Bottom: schematic representation of spin configurations.

state may have only two magnetizations:  $M_1 = s$  and  $-s$  (see inset), i.e.,  $q = 0$  and  $2s$ , leading just to  $|m| = 1, 0$  plateaus. For  $n = 2$  and  $j_z > 0$ , the GS possesses plateaus at  $|m| = 1, \frac{1}{2}$  (top right), reflecting the magnetizations  $M_3 = \frac{3}{2}, \frac{1}{2}$  ( $q = 0, 1$ ) of the trimer formed by the three spins trapped between two aligned spins. Moreover, the trimer cannot reach  $M_3 = -\frac{1}{2}$  (except for large  $h_2 \approx -h_1$ ) entailing no wide  $m = 0$  plateau. For  $n = 3$ , however, pentamer magnetization  $M_5$  does reach  $-\frac{1}{2}$ , entailing a large  $m = 0$  plateau, in addition to the aligned phase  $|m| = 1$  ( $M_5 = \frac{5}{2}$ ,  $q = 0$ ) and smaller intermediate plateaus at  $|m| = \frac{2}{3}, \frac{1}{3}$  ( $M_5 = \frac{3}{2}, \frac{1}{2}$ ,  $q = 1, 2$ , bottom left). Such persistent plateaus also occur for higher spins, as seen for  $s = 1$  and  $n = 2$  (bottom right), where  $|m| = 1, \frac{3}{4}, \frac{1}{2}, \frac{1}{4}$ , following the trimer magnetizations  $M_3 = 3, 2, 1, 0$ .

Figure 5 shows the single-spin magnetization  $\langle S_i^z \rangle$  of the first four spins in the chains of Fig. 3. For  $s = \frac{1}{2}$ ,  $\frac{1}{2} - |\langle S_i^z \rangle|$  is also a measure of the *entanglement* of spin  $i$  with the rest of the chain (i.e., of the mixedness of the single spin-reduced state [77]), with  $|\langle S_i^z \rangle| = 0$  ( $\frac{1}{2}$ ) implying maximum (zero)  $i$ -rest entanglement.

The spins with field will align with the field direction as  $h_i$  increases, leading for  $n = 1$  to type-a (-b) spin configurations for strong parallel (antiparallel) fields. However, those without field ( $n \geq 2$ ) exhibit a more complex behavior. For  $n = 2$  and  $j_z = 0$ , the total GS magnetization  $M$  vanishes  $\forall h_1, h_2$ , implying that these spins become *antialigned* for  $h_1 = h_2$ , leading to a type-b Néel configuration, but have *zero magnetization* ( $\langle S_i^z \rangle = 0$ ) for  $h_1 = -h_2$ , entailing a type-d configuration. This configuration also holds for  $j_z > 0$  if  $h_1 = -h_2$  (and  $|h_i| > h_s$  if  $j_z > j$ ) since  $M$  still vanishes, implying that these spins become *frustrated*, as the attractive  $S_i^z S_{i+1}^z$  coupling cannot be satisfied with both adjacent spins.

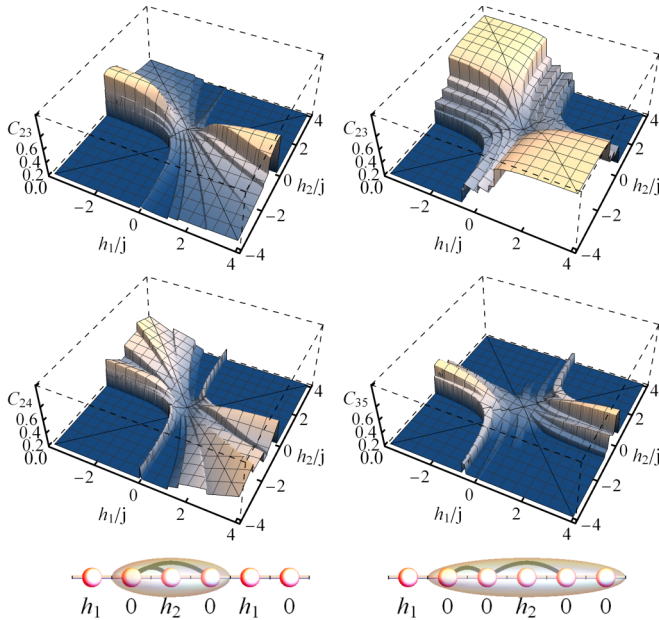


FIG. 6. Concurrence  $C_{ij}$  between spins  $i$  and  $j$  (joined by a line in the bottom row) in the  $(h_1, h_2)$  field space for the exact GS of an  $N = 12$ ,  $s = \frac{1}{2}$  chain with  $j_z/j = 0.75$ , in NA (left) and NNA (right) field configurations. The steps reflect the different total chain magnetizations. The onset of entanglement is determined by the border of the aligned phase. Bottom: schematic representation of approximate trimerization occurring in the  $\pm N/4$  plateaus for  $n = 2$ , and pentamerization in the  $\pm N/3$  and  $\pm N/6$  plateaus for  $n = 3$ .

This is a clear example of *field-induced frustration*, and entails *maximum  $i$ -rest entanglement*, mostly saturated with neighboring zero field spins. On the other hand, for large  $h_1 = h_2$  and  $j_z > 0$ , they become aligned (type a).

In contrast, for  $n = 3$  the two contiguous spins without field tend to form an *entangled dimer*, leading for  $j_z = 0$  to a type-e configuration ( $\langle S_i^z \rangle \approx 0$  for  $i = 2, 3$ ) if  $h_1 = h_2$  and a type-f configuration if  $h_1 = -h_2$ , here slightly polarized towards b. In this case, there is actually a spin configuration transition when  $0 < j_z < j_z^c(3) = j/2$ , where  $\langle S_i^z \rangle$  changes sign at the central spins and the polarization evolves from type b to type c, crossing exactly type f. For  $j_z > j/2$ , these central spins remain significantly entangled for antiparallel fields, polarized towards type c, while for parallel fields they become increasingly aligned as  $|h_i|$  and hence  $|M|$  increases. Previous behaviors can also be seen at the bottom panels for  $j_z > j$ , which depict the “evolution” of  $\langle S_i^z \rangle$  with  $\theta = \tan^{-1}(-h_2/h_1)$  between the fully aligned phases.

### C. Pairwise entanglement

We show in Fig. 6 illustrative results for the pairwise entanglement measured through the concurrence [72], in the chains of Fig. 3 for  $j_z/j = 0.75$ . It is first verified that in the  $n = 3$  NNA case, the two contiguous spins with zero field ( $C_{23}$ , top right) are highly entangled in the  $M = 0$  plateau since the spins form there essentially a type-f dimerized configuration (see bottom row of Fig. 5). Accordingly, the concurrence  $C_{35}$  of a noncontiguous pair with zero field spins (bottom right) vanishes in this plateau. In contrast, the latter becomes

significant in the  $|M| = 4$  and  $|M| = 2$  plateaus ( $|m| = \frac{2}{3}, \frac{1}{3}$ ), where the intermediate field  $h_2$  is weak, in agreement with the pentamerization argument.

On the other hand, in the  $n = 2$  NA case,  $C_{23}$  (spin without field and spin with field  $h_2$ , top left) is clearly significant in the  $|M| = N/4$  plateaus emerging for small  $|h_2|$ , and small or zero in the same plateaus emerging for small  $|h_1|$  and strong  $|h_2|$ , supporting the trimerization argument. This is verified in  $C_{24}$  (bottom left), which is also significant (zero) when  $C_{23}$  is large (small) in these plateaus, entailing essentially no entanglement between trimers.  $C_{24}$  is also non-negligible at the  $M = 0$  plateau, where nearest spins with no field become entangled due to the field-induced frustration. It is also confirmed that all concurrences are finite at the  $|M| = Ns - 1$  band, in agreement with Eq. (19).

## III. CONCLUSIONS

We have shown that  $n$ -alternating field configurations can lead to GS phase diagrams which differ significantly from those of the standard alternating case. They can exhibit non-trivial magnetization plateaus associated with field-induced frustration and polymerization phenomena, which persist for large sizes as verified by DMRG calculations. These plateaus satisfy a quantization rule compatible with the OYA criterion and are shown to stem from field-induced polymers with definite magnetization, where spins trapped between spins with fields become highly entangled among themselves but are essentially disentangled with spins in another polymer. Exact analytic expressions for the boundary in field space of the fully aligned phase, valid for all  $n$ , were also derived, and imply a critical  $n$ -dependent anisotropy  $j_z^c(n)/j$  below which the aligned phase together with a whole interval of GS magnetizations become unreachable even for arbitrarily strong fields. The boundary of the aligned phase represents in addition the onset of GS entanglement (as well that of the symmetry-breaking phase at the mean field level), with pairwise entanglement acquiring there full range. These results open possibilities for applications of finite chains with simple interactions under controllable fields, such as entanglement tuning and plateau formation at rational values of the scaled magnetization, and pave the way to study the emergence of critical phenomena induced through nonuniform fields within more general architectures and couplings.

## ACKNOWLEDGMENTS

We thank Dr. J. M. Matera for useful discussions. The authors acknowledge support from CONICET (M.C., N.C., and C.A.L.) and CIC (R.R.) of Argentina.

## APPENDIX A: BORDER OF THE ALIGNED PHASE IN THE $n$ -ALTERNATING SPIN- $s$ XXZ SYSTEM

We first prove Eqs. (8) and (9). In the standard alternating case  $n = 1$ ,  $\Delta H_n$  in (15) is just a  $2 \times 2$  matrix

$$\Delta H_1 = \begin{pmatrix} h_1 + j_z & -j \\ -j & h_2 + j_z \end{pmatrix}, \quad (\text{A1})$$

and a trivial calculation yields  $a_1 = 1$ ,  $b_1 = j_z$ , and  $c_1 = j_z^2 - j^2$  in (16), with  $\alpha_1 = j$ ,  $\beta_1 = j_z$  [Eq. (20)]. In this case, the lowest eigenvalue of  $\Delta H_n$  is just  $\lambda_0(1) = j_z + \frac{h_1+h_2}{2} - \sqrt{(\frac{h_1-h_2}{2})^2 + j^2}$ , and Eq. (6) can be directly obtained from the condition  $\lambda_0(1) > 0$ .

For general  $n \geq 2$ , evaluation of  $\text{Det}[\Delta H_n]$  in Eq. (16) yields

$$a_n = (d_{n-1})^2, \quad b_n = d_{2n-1}, \quad (\text{A2})$$

and  $c_n = d_{2n} - \frac{j^2}{4}d_{2n-2} - 2\frac{j^{2n}}{4^n}$ , where

$$d_n = \begin{vmatrix} j_z & -j/2 & 0 & 0 & \dots \\ -j/2 & j_z & -j/2 & 0 & \dots \\ & & \ddots & & \\ & & & \ddots & \\ 0 & \dots & 0 & -j/2 & j_z \end{vmatrix} \quad (\text{A3})$$

is the determinant of an  $n \times n$  Toeplitz [78] tridiagonal matrix  $M_n$  of elements  $j_z \delta_{ij} - \frac{j}{2} \delta_{i,j \pm 1}$ . It then satisfies

$$d_{n+1} = j_z d_n - (j/2)^2 d_{n-1} \quad (\text{A4})$$

for  $n \geq 1$ , with  $d_1 = j_z$ ,  $d_0 \equiv 1$ , i.e.,  $(d_n^{j_z}) = A^n(j_z)$ , with  $A = (j_z - j^2/4)$ . Hence, for any  $n \geq 1$ , diagonalization of  $A$ , which has eigenvalues  $\frac{1}{2}(j_z \pm h_s) = \frac{j}{2}e^{\pm\gamma}$ , with  $h_s = \sqrt{j_z^2 - j^2} = j \sinh \gamma$  and  $\cosh \gamma = j_z/j$ , leads to

$$d_n = \frac{(j_z + h_s)^{n+1} - (j_z - h_s)^{n+1}}{2^{n+1}h_s} = \frac{j^n \sinh[(n+1)\gamma]}{2^n \sinh \gamma}. \quad (\text{A5})$$

Equations (A2)–(A5) then lead to  $a_n = (\frac{j}{2})^{2n-2} \frac{\sinh^2 n\gamma}{\sinh^2 \gamma}$ ,  $b_n = (\frac{j}{2})^{2n-1} \frac{\sinh 2n\gamma}{\sinh \gamma}$ , and  $c_n = 4(\frac{j}{2})^{2n} \sinh^2 n\gamma$ , implying  $\alpha_n = 2(\frac{j}{2})^n/d_{n-1}$ , i.e., Eq. (8), with  $\beta_n = b_n/a_n$  given by (9). ■

Now, it is apparent from (16) and previous expressions that the matrix  $\Delta H_n$  is positive definite for  $j_z > j$  and positive fields  $h_1, h_2$  ( $a_n > 0$ ,  $b_n > 0$ ,  $c_n > 0 \forall$  real  $\gamma$ ). On the other hand, at the threshold value (5),  $\gamma = i\pi/n$  and Eqs. (A2)–(A5) lead to  $a_n = b_n = c_n = 0$ , i.e.,  $\text{Det}[\Delta H_n] = 0 \forall h_1, h_2$ , indicating the presence of a *vanishing* eigenvalue of  $\Delta H_n$  and hence the loss of stability of the aligned  $M = Ns$  GS.

The eigenvalues of  $\Delta H_n$  represent of course excitation energies constructed from single-spin excitations when  $\Delta H_n$  is positive definite. The eigenvalue equation  $\text{Det}[\Delta H_n - \lambda \mathbb{1}] = 0$  can be explicitly obtained from Eq. (16) and the previous expressions for  $a_n, b_n, c_n$ , replacing  $j_z \rightarrow j_z - \lambda$  and  $\gamma \rightarrow i\phi$ . It reads as

$$\left(\frac{j}{2}\right)^{2n-2} \frac{\sin^2 n\phi}{\sin^2 \phi} \left[ h_1 h_2 + \frac{j(h_1 + h_2) \sin \phi}{\tan n\phi} - j^2 \sin^2 \phi \right] = 0, \quad (\text{A6})$$

where  $\cos \phi = (j_z - \lambda)/j$ . It is first seen that (A6) is fulfilled for  $\phi = \pi k/n$ ,  $k = 1, \dots, n-1$ , implying the  $n-1$  *field-independent* eigenvalues

$$\lambda_k(n) = j_z - j \cos(\pi k/n), \quad k = 1, \dots, n-1. \quad (\text{A7})$$

The lowest one,  $\lambda_1(n)$ , vanishes precisely at the threshold (5), becoming negative for  $j_z < j_z^c(n) = j \cos(\pi/n)$ . In addition, the brackets in (A6) lead to the remaining  $n+1$

*field-dependent* eigenvalues. The lowest one is obtained for  $\phi = \phi_0 < \pi/n$  (and  $\phi_0 > 0$ ), leading to

$$\lambda_0(n) = j_z - j \cos \phi_0 < \lambda_1(n) = j_z - j \cos \pi/n, \quad (\text{A8})$$

with equality approached only at strong fields  $h_1, h_2 \gg j$  [where  $\phi_0 \approx \pi/n - \frac{h_1+h_2}{nh_1h_2} \sin(\pi/n)$ , approaching  $\pi/n$  for  $h_1, h_2 \rightarrow +\infty$ ]. Thus, for  $j_z > j_z^c(n)$ ,  $\Delta H_n$  is always positive definite at sufficiently strong fields [ $\lambda_0(n) > 0$ ], while for  $j_z \leq j_z^c(n)$ , it is nonpositive [ $\lambda_0(n) < 0$ ] at all finite fields and the aligned state can no longer be a GS.

Replacing  $j_z \rightarrow j_z - \lambda$  in (A5), it is also seen that the eigenvalues of the  $(n-1) \times (n-1)$  Toeplitz matrix  $M_{n-1}$  are just those of Eq. (A7) [78]. This matrix is just the block of  $(\Delta H)_n$  associated with the  $n-1$  contiguous spins with no field, which become decoupled from the aligned spins with field for  $h_1, h_2 \rightarrow \infty$ . Hence,  $-j \cos \pi/n$  represents the lowest energy of the  $n-1$  spins trapped between the two aligned spins at  $j_z = 0$  and magnetization  $(n-1)s - 1$ .

While a positive-definite matrix  $\Delta H_n$  is in principle a necessary condition for stability of the  $M = Ns$  GS, it turns out to be sufficient for  $h_1 + h_2 > 0$  since in this case the GS magnetization decreases in steps of length 1 from its maximum  $M = Ns$  as the fields  $h_1, h_2$  decrease from  $+\infty$  (Fig. 3). The only exception occurs for  $j_z > j$  along the line  $h_1 + h_2 = 0$  between the factorizing fields (see bottom panels in Fig. 3), where the aligned states  $M = \pm Ns$  become degenerate GS's if  $|h_i| < h_s$ , and all GS magnetization plateaus merge if  $|h_i| = h_s$ .

Finally, we note that in the mean field approximation, the onset of the symmetry-breaking phase is again determined by the fields where the matrix  $\Delta H_n$  ceases to be positive definite since it is constructed from single-spin excitations. A symmetry-breaking product state  $|\Psi_{\text{mf}}\rangle \propto e^{-i \sum_i \theta_i S_i^y} |M = Ns\rangle$  becomes in fact  $\approx |Ns\rangle + \sum_i w_i |W_i\rangle$  for small  $\theta_i$ , with  $w_i = \theta_i \sqrt{sK/2}$ . Hence, a nonpositive  $\langle \Psi_{\text{mf}} | \Delta H | \Psi_{\text{mf}} \rangle$  is then equivalent to  $\Delta H_n$  not being positive definite.

## APPENDIX B: REDUCED STATES AND ENTANGLEMENT IN THE $M = Ns - 1$ GS

The  $|M = Ns - 1\rangle$  GS will have the form

$$|Ns - 1\rangle = \sum_{i=1}^{2n} w_i |W_i\rangle, \quad (\text{B1})$$

where  $|W_i\rangle$  are the states (12) and the coefficients  $w_i$  are obtained from the diagonalization of the matrix  $\Delta H_n$  of elements (14) ( $\sum_i |w_i|^2 = 1$ , with  $w_i > 0 \forall i$  for  $J > 0$ ). From the form (12) of the states  $|W_i\rangle$ , it becomes apparent that the reduced state  $\rho_{kl} = \text{Tr}_{\bar{k}l} |Ns - 1\rangle \langle Ns - 1|$  of any two distinct spins  $k \neq l$  in the state (B1) will depend just on their positions  $i, j$  within the cell each spin belongs, but not on their absolute distance  $|k - l|$ . Since the reduced state will also commute with the total spin  $S_{kl}^z = S_k^z + S_l^z$  of the pair, it will be given, for  $M = Ns - 1$ , by ( $K = N/2n$  is the number of cells)

$$\rho_{ij} = \begin{pmatrix} 1 - \frac{|w_i|^2 + |w_j|^2}{K} & 0 & 0 & 0 \\ 0 & \frac{|w_j|^2}{K} & \frac{w_j w_i^*}{K} & 0 \\ 0 & \frac{w_i w_j^*}{K} & \frac{|w_i|^2}{K} & 0 \\ 0 & 0 & 0 & 0 \end{pmatrix} \quad (\text{B2})$$

in the subspace spanned by the states  $\{|s, s\rangle, |s, s-1\rangle, |s-1, s\rangle, |s-1, s-1\rangle\}$ , where  $|s-1\rangle = \frac{1}{\sqrt{2s}}S^-|s\rangle$ . Equation (B2) is valid for any  $s$  and  $i, j = 1, \dots, 2n$ . It can then be always considered as a mixed state of an *effective two-qubit system*, as just states  $|s\rangle$  and  $|s-1\rangle$  are involved at each spin. A similar expression holds for the reduced state in the  $M = -Ns + 1$  GS in the corresponding subspace.

The state (B2) is a mixed state with two nonzero eigenvalues  $p_{ij} = (|w_i|^2 + |w_j|^2)/K$  and  $1 - p_{ij}$ . Its entropy  $S(\rho_{ij}) = -\text{Tr} \rho_{ij} \log_2 \rho_{ij}$  is the entanglement entropy of the pair with the rest of the chain. On the other hand, the entanglement between both spins can be measured through its entanglement of formation [71], defined as the convex roof extension of the pure state entanglement entropy. For a general mixed state  $\rho \equiv \rho_{AB}$ , it is the minimum of the average entanglement over all decompositions of  $\rho$  as convex mixture of pure states:

$$E_f(\rho) = \text{Min}_{\{q_\alpha, |\Psi_\alpha\rangle\}} \sum_\alpha q_\alpha E(|\Psi_\alpha\rangle), \quad (\text{B3})$$

where  $\sum_\alpha q_\alpha |\Psi_\alpha\rangle\langle\Psi_\alpha| = \rho$ ,  $q_\alpha \geq 0$ ,  $\sum_\alpha q_\alpha = 1$ , and  $E(|\Psi_\alpha\rangle) = S(\rho_A^\alpha) = S(\rho_B^\alpha)$  is the entanglement entropy of  $|\Psi_\alpha\rangle$  ( $\rho_{A(B)}^\alpha = \text{Tr}_{B(A)} |\Psi_\alpha\rangle\langle\Psi_\alpha|$  are the reduced states).

While the evaluation of Eq. (B3) in the general case is a computationally hard problem, for a two-qubit mixed state  $\rho$  it can be analytically determined through the concurrence  $C(\rho)$  [72], defined as in Eq. (B3) with  $E(|\Psi_\alpha\rangle) \rightarrow C(|\Psi_\alpha\rangle) = \sqrt{S_2(\rho_A^\alpha)} = \sqrt{S_2(\rho_B^\alpha)}$ , where  $S_2(\rho) = 2(1 - \text{Tr} \rho^2)$  is the linear entropy. For a two-qubit state  $\rho$ , the concurrence can be calculated as [72]

$$C(\rho) = \text{Max}[2\lambda_{\text{max}} - \text{Tr} R, 0], \quad R = [\rho^{1/2} \tilde{\rho} \rho^{1/2}]^{1/2}, \quad (\text{B4})$$

where  $\lambda_{\text{max}}$  denotes the largest eigenvalue of  $R$  and  $\tilde{\rho} = \sigma_y \otimes \sigma_y \rho^* \sigma_y \otimes \sigma_y$  is the spin-flipped density, with  $\sigma_y$  the Pauli matrix. Equation (B3) then becomes [72]

$$E_f(\rho) = - \sum_{v=\pm} q_v \log_2 q_v, \quad q_{\pm} = \frac{1 \pm \sqrt{1 - C^2(\rho)}}{2}, \quad (\text{B5})$$

and is just an increasing convex function of  $C(\rho)$ , with  $E_f(\rho) = C(\rho) = 1$  (0) for a maximally entangled (separable) two-qubit state. For a pure state  $\rho = |\Psi\rangle\langle\Psi|$ ,  $C(\rho) = \sqrt{S_2(\rho_{A(B)})}$  and  $E_f(\rho)$  becomes the standard entanglement entropy  $S(\rho_{A(B)})$ . The concurrence is itself a proper entanglement monotone [73] and satisfies a monogamy inequality [74,75].

In the case of the state (B2), the pair concurrence  $C_{ij} = C(\rho_{ij})$  obtained from Eq. (B4) becomes just  $C_{ij} = 2|(\rho_{ij})_{23}| = 2|w_i w_j|/K$  and is then given by Eq. (19). These concurrences saturate the monogamy inequality, namely,

$$\sum_{l \neq i} C_{il}^2 = 4 \frac{|w_i|^2}{K} \left(1 - \frac{|w_i|^2}{K}\right) = C_{i,\text{rest}}^2, \quad (\text{B6})$$

where  $C_{i,\text{rest}}^2 = S_2(\rho_i) = 2(1 - \text{Tr} \rho_i^2)$  is the tangle of single spin  $i$  with the rest of the chain, with

$$\rho_i = \begin{pmatrix} 1 - |w_i|^2/K & 0 \\ 0 & |w_i|^2/K \end{pmatrix}, \quad (\text{B7})$$

the reduced state of spin  $i$  in the state (B2). For a general state we have instead  $\sum_{l \neq i} C_{il}^2 \leq C_{i,\text{rest}}^2$  [74,75].

While Eq. (19) is valid for any spin  $s$  due to the form (B2) of the reduced pair state, in general states the pairwise entanglement of formation for spin  $s \geq 1$  will not be analytically computable. Instead, we can use as computable quantifier the negativity  $N(\rho)$  [79], defined as the absolute value of the sum of the negative eigenvalues of the partial transpose of  $\rho \equiv \rho_{AB}$ . According to the Peres criterion [80],  $N(\rho) > 0$  implies entanglement (although the converse does not hold in general). In the  $|M| = Ns - 1$  region, the negativity  $N_{ij} = N(\rho_{ij})$  determined by the state (B2) is, setting  $\gamma_{ij} = 1 - (|w_i|^2 + |w_j|^2)/K$ ,

$$N_{ij} = \frac{1}{2} \left( \sqrt{\gamma_{ij}^2 + 4|w_i|^2|w_j|^2/K^2} - \gamma_{ij} \right), \quad (\text{B8})$$

with  $N_{ij} \rightarrow C_{ij}^2/2$  for large  $K$ .

Due to the symmetry  $w_{n+1+i} = w_{n+1-i}$  valid for  $i = 1, \dots, n-1$  in the exact GS under cyclic conditions, the coefficients  $w_i$  in (B1) can be obtained by diagonalizing an effective  $(n+1) \times (n+1)$  matrix  $\Delta H'_n$ . Altogether there are just  $(n+1)$  distinct coefficients  $w_i$  and hence just  $(n+1)(n+2)/2$  distinct pairwise concurrences and negativities for general  $h_1, h_2$  in the  $|M| = Ns - 1$  GS.

### APPENDIX C: EXACT SOLUTION OF THE XX CHAIN IN $n$ -ALTERNATING FIELD CONFIGURATIONS

When  $J_z = 0$ , the XXZ model reduces to the XX model. For  $s = \frac{1}{2}$ , the ensuing Hamiltonian can be mapped exactly to a bilinear fermionic form in the annihilation  $c_j^\dagger$  and creation  $c_j$  operators by means of the Jordan-Wigner transformation [2]  $c_j^\dagger = S_j^+ \exp(-i\pi \sum_{k=1}^{j-1} S_k^+ S_k^-)$  for each value of the fermionic number parity (i.e., the  $S_z$  parity)

$$P \equiv \exp(i\pi \mathbf{N}) = \sigma = \pm 1, \quad (\text{C1})$$

where  $\mathbf{N} = \sum_{j=1}^N c_j^\dagger c_j = S^z + N/2$  is the fermion number operator. This leads to

$$H = - \sum_j \left[ h_j (c_j^\dagger c_j - 1/2) - \eta_j^\sigma \frac{J}{2} (c_{j+1}^\dagger c_j + c_j^\dagger c_{j+1}) \right], \quad (\text{C2})$$

where, for cyclic conditions,  $\eta_j^- = 1 \forall j$  and  $\eta_j^+ = 1 (-1)$  for  $j \leq N-1$  ( $j = N$ ). After a discrete Fourier transform of the fermion operators, it can be expressed as a sum of  $K$   $2n \times 2n$  matrices  $\mathbf{H}_k$ :

$$H = - \sum_{k=1-\delta_{\sigma 1/2}}^{K-\delta_{\sigma 1/2}} \mathbf{c}_k^\dagger \cdot \mathbf{H}_k \mathbf{c}_k - \epsilon, \quad (\text{C3})$$

$$\mathbf{H}_k = \begin{pmatrix} h^+ + J \cos \omega_k & h^- & \dots \\ h^- & h^+ + J \cos(\omega_k + \frac{\pi}{n}) & \dots \\ \vdots & \vdots & \ddots \end{pmatrix} \quad (\text{C4})$$

$$= \mathbf{D}_k + \mathbf{A}, \quad (\text{C5})$$

with  $\mathbf{c}_k^\dagger = (c_k^\dagger, c_{k+N/(2n)}^\dagger, \dots, c_{k+(2n-1)N/(2n)}^\dagger)$ ,  $\mathbf{D}_k$  a diagonal matrix of elements  $(\mathbf{D}_k)_{ii} = J \cos(\omega_k + \frac{\pi(i-1)}{n})$ ,  $\mathbf{A}$  a

circulant matrix specified by the vector  $(h^+, h^-, h^+, h^-, \dots)$ , and

$$h^\pm = \frac{h_1 \pm h_2}{2n}, \quad \epsilon = \frac{Nh^+}{2}, \quad \omega_k = 2\pi k/N. \quad (\text{C6})$$

Equation (C3) shows that the Fourier-transformed  $n$ -alternating field configuration leads to off-diagonal hopping terms specifying the allowed momentum values. The index  $k$  is half-integer (integer) for  $\sigma = 1$  ( $-1$ ).

Due to the parity dependence of the energy levels, the number of GS magnetization transitions is associated to the number of times the single-particle energies change sign [83]. Hence, field values at which single-particle energies vanish can be determined by solving

$$\text{Det}(\mathbf{H}_k) = 0, \quad (\text{C7})$$

with  $k = \frac{1}{2}, 1, \dots, K$ .

For standard alternating fields  $n = 1$ , Eq. (C4) becomes

$$\mathbf{H}_k = \begin{pmatrix} h^+ + J \cos \omega_k & h^- \\ h^- & h^+ - J \cos \omega_k \end{pmatrix}, \quad (\text{C8})$$

yielding the well-known single-particle energies [81–87]

$${}_1\lambda_k^\pm = h^+ \pm \sqrt{(h^-)^2 + J^2 \cos^2 \omega_k}. \quad (\text{C9})$$

In this case,

$$\text{Det}(\mathbf{H}_k) = h_1 h_2 - J^2 \cos^2 \omega_k, \quad (\text{C10})$$

and Eq. (C7) determines  $N/2$  hyperbolas in the  $(h_1, h_2)$  field space, meaning that the GS will then exhibit definite magnetization plateaus ranging from  $|M| = 0$  to  $|M| = N/2$ . In particular, for  $k = N/2$  the lowest  $\sigma = -1$  parity level becomes negative and we recover *exactly* the hyperbola  $h_1 h_2 = j^2$  of the  $N/2 \rightarrow N/2 - 1$  transition, in agreement with Eqs. (6)

and (7) for  $n = 1$  and  $j_z = 0$ . For  $n \geq 2$ , the expressions for the eigenvalues are more involved.

In the NA  $n = 2$  case, the determinant of  $\mathbf{H}_k$  is

$$\text{Det}(\mathbf{H}_k) = \frac{J^4}{4} \sin^2(2\omega_k), \quad (\text{C11})$$

which becomes zero only for  $k = N/4$  and implies at least one identically zero single-particle energy. The latter means that there is no single-particle energy which changes sign as the fields are varied and indicates that there should be no GS magnetization transition. Furthermore, we now prove the following lemma:

*Lemma 1.* The GS of a finite XX spin system in a  $n = 2$  next-alternating field configuration is a nondegenerate half-filled state with definite magnetization  $M = 0$ ,  $\forall h_1, h_2$ .

*Proof.* We first start by comparing the number of energy levels with negative single-particle energies within each parity  $\sigma$  and their ensuing lowest energy  $E_\sigma$ . Since  $\text{Det}[\mathbf{H}_k] \geq 0 \forall k$  [Eq. (C11)], then each matrix  $\mathbf{H}_k$  is either positive (or negative) semidefinite, or it has two positive and two negative eigenvalues. However, since the determinant of any leading principal minor connecting  $i$  with  $i + 2$  is  $-J^2 \cos^2(\omega_k)$ ,  $\mathbf{H}_k$  cannot be positive or negative semidefinite. In the  $\sigma = 1$  subspace,  $\text{Det}[\mathbf{H}_k] > 0 \forall k = \{\frac{1}{2}, \dots, K - 1/2\}$ , entailing that there are always  $N/2 = 2K$  negative single-particle energies, whereas for  $\sigma = -1$  there are  $N/2 - 1$ , as one of the eigenvalues of  $\mathbf{H}_{N/4}$  is identically zero. Due to this small, albeit important, difference in the number of negative energy levels,  $E_1 < E_{-1} \forall h_1, h_2$ . While this result can be numerically verified, for  $h_2 = \pm h_1 = \pm h$  a series expansion of the energy difference between the lowest energies of each parity,  $\Delta E = E_{-1} - E_1$ , shows that  $\Delta E > 0 \forall h$ . Likewise, for strong fields a second-order perturbation treatment in the couplings shows that the  $M = 0$  eigenstate is the GS  $\forall J$ . ■

- 
- [1] S. Sachdev, *Quantum Phase Transitions* (Cambridge University Press, Cambridge, England, 1999); *Nat. Phys.* **4**, 173 (2008).
- [2] E. Lieb, T. Schultz, and D. Mattis, *Ann. Phys. (NY)* **16**, 407 (1961).
- [3] M. Vojta, *Rep. Prog. Phys.* **66**, 2069 (2003).
- [4] N. Laflorencie, I. Affleck, and M. Berciu, *J. Stat. Mech.* (2005) P12001.
- [5] Z. Wang, T. Lorenz, D. I. Gorbunov, P. T. Cong, Y. Kohama, S. Niesen, O. Breunig, J. Engelmayer, A. Herman, J. Wu, K. Kindo, J. Wosnitza, S. Zherlitsyn, and A. Loidl, *Phys. Rev. Lett.* **120**, 207205 (2018).
- [6] A. Osterloh, L. Amico, G. Falci, and R. Fazio, *Nature (London)* **416**, 608 (2002).
- [7] T. J. Osborne and M. A. Nielsen, *Phys. Rev. A* **66**, 032110 (2002).
- [8] G. Vidal, J. I. Latorre, E. Rico, and A. Kitaev, *Phys. Rev. Lett.* **90**, 227902 (2003).
- [9] A. R. Its, B.-Q. Jin, and V. E. Korepin, *J. Phys. A: Math. Gen.* **38**, 2975 (2005).
- [10] L. Amico, R. Fazio, A. Osterloh, and V. Vedral, *Rev. Mod. Phys.* **80**, 517 (2008).
- [11] J. Eisert, M. Cramer, and M. B. Plenio, *Rev. Mod. Phys.* **82**, 277 (2010).
- [12] J. Stasinska, B. Rogers, M. Paternostro, G. De Chiara, and A. Sanpera, *Phys. Rev. A* **89**, 032330 (2014).
- [13] N. Blanc, J. Trinh, L. Dong, X. Bai, A. A. Aczel, M. Mourigal, L. Balents, T. Siegrist, and A. P. Ramirez, *Nat. Phys.* **14**, 273 (2018).
- [14] C. Lacroix, P. Mendels, and F. Mila, *Introduction to Frustrated Magnetism: Materials, Experiments, Theory* (Springer, Berlin, 2013).
- [15] A. Sen(De), U. Sen, J. Dziarmaga, A. Sanpera, and M. Lewenstein, *Phys. Rev. Lett.* **101**, 187202 (2008).
- [16] F. Michaud, T. Coletta, S. R. Manmana, J. D. Picon, and F. Mila, *Phys. Rev. B* **81**, 014407 (2010).
- [17] S. M. Giampaolo, G. Gualdi, A. Monras, and F. Illuminati, *Phys. Rev. Lett.* **107**, 260602 (2011); U. Marzolino, S. M. Giampaolo, and F. Illuminati, *Phys. Rev. A* **88**, 020301(R) (2013).
- [18] A. Honecker, J. Schulenburg, and J. Richter, *J. Phys.: Condens. Matter* **16**, S749 (2004).
- [19] A. Tanaka, K. Totsuka, and X. Hu, *Phys. Rev. B* **79**, 064412 (2009).

- [20] M. Takigawa and F. Mila, *Magnetization Plateaus*, Springer Series in Solid-State Sciences (Springer, Berlin, 2011), Vol. 164, Chap. 10, pp. 241–267.
- [21] C. A. Lamas, S. Capponi, and P. Pujol, *Phys. Rev. B* **84**, 115125 (2011); F. Elias, M. Arlego, and C. A. Lamas, *ibid.* **95**, 214426 (2017).
- [22] H. Hu, C. Cheng, Z. Xu, H.-G. Luo, and S. Chen, *Phys. Rev. B* **90**, 035150 (2014).
- [23] M. Oshikawa, M. Yamanaka, and I. Affleck, *Phys. Rev. Lett.* **78**, 1984 (1997).
- [24] H. Zhang, C. A. Lamas, M. Arlego, and W. Brenig, *Phys. Rev. B* **93**, 235150 (2016).
- [25] C. K. Majumdar and D. K. Ghosh, *J. Math. Phys.* **10**, 1399 (1969).
- [26] S. Nishimoto, N. Shibata, and C. Hotta, *Nat. Commun.* **4**, 2287 (2013).
- [27] F. C. Alcaraz and A. L. Malvezzi, *J. Phys. A: Math. Gen.* **28**, 1521 (1995).
- [28] M. Asoudeh and V. Karimipour, *Phys. Rev. A* **71**, 022308 (2005).
- [29] G.-F. Zhang and S.-S. Li, *Phys. Rev. A* **72**, 034302 (2005).
- [30] N. Canosa, R. Rossignoli, and J. M. Matera, *Phys. Rev. B* **81**, 054415 (2010).
- [31] S. Mahdaviifar and J. Abouie, *J. Phys.: Condens. Matter* **23**, 246002 (2011).
- [32] A. A. Zvyagin, *Phys. Rev. B* **97**, 214425 (2018); *Quantum Theory of One-Dimensional Spin Systems* (Cambridge University Press, Cambridge, UK, 2010).
- [33] C. Li, G. Zhang, and Z. Song, *Phys. Rev. A* **94**, 052113 (2016).
- [34] T. Chanda, T. Das, D. Sadhukhan, A. K. Pal, A. Sen De, and U. Sen, *Phys. Rev. A* **94**, 042310 (2016).
- [35] M. Cerezo, R. Rossignoli, and N. Canosa, *Phys. Rev. B* **92**, 224422 (2015); *Phys. Rev. A* **94**, 042335 (2016).
- [36] M. Cerezo, R. Rossignoli, N. Canosa, and E. Ríos, *Phys. Rev. Lett.* **119**, 220605 (2017).
- [37] M. Lewenstein, A. Sanpera, and V. Ahufinger, *Ultracold Atoms in Optical Lattices: Simulating Quantum Many-Body Systems* (Oxford University Press, New York, 2012).
- [38] I. M. Georgescu, S. Ashhab, and F. Nori, *Rev. Mod. Phys.* **86**, 153 (2014).
- [39] *Principles and Methods of Quantum Information Technologies*, edited by Y. Yamamoto and K. Semba (Springer, New York, 2016).
- [40] C. N. Yang and C. P. Yang, *Phys. Rev.* **150**, 321 (1966).
- [41] J. D. Johnson and M. McCoy, *Phys. Rev. A* **6**, 1613 (1972).
- [42] F. C. Alcaraz, S. R. Salinas, and W. F. Wreszinski, *Phys. Rev. Lett.* **75**, 930 (1995); F. C. Alcaraz, A. Saguia, and M. S. Sarandy, *Phys. Rev. A* **70**, 032333 (2004).
- [43] D. V. Dmitriev, V. Y. Krivnov, and A. A. Ovchinnikov, *Phys. Rev. B* **65**, 172409 (2002); D. V. Dmitriev, V. Y. Krivnov, A. A. Ovchinnikov, and A. Langari, *Zh. Eksp. Teor. Fiz.* **122**, 624 (2002) [*J. Exp. Theor. Phys.* **95**, 538 (2002)].
- [44] S.-J. Gu, H.-Q. Lin, and Y.-Q. Li, *Phys. Rev. A* **68**, 042330 (2003).
- [45] N. Canosa and R. Rossignoli, *Phys. Rev. A* **73**, 022347 (2006); E. Ríos, R. Rossignoli, and N. Canosa, *J. Phys. B: At., Mol. Opt. Phys.* **50**, 095501 (2017).
- [46] R. Jafari and A. Langari, *Phys. Rev. B* **76**, 014412 (2007).
- [47] O. Breunig, M. Garst, E. Sela, B. Buldmann, P. Becker, L. Bohatý, R. Müller, and T. Lorenz, *Phys. Rev. Lett.* **111**, 187202 (2013).
- [48] J. Reisons, E. Mascarenhas, and V. Savona, *Phys. Rev. B* **96**, 165137 (2017).
- [49] J. Ren, Y. Wang, and W. L. You, *Phys. Rev. A* **97**, 042318 (2018).
- [50] G. Xu and G. Long, *Sci. Rep.* **4**, 6814 (2014).
- [51] Y. Salathe, M. Mondal, M. Oppliger, J. Heinsoo, P. Kurpiers, A. Potocnik, A. Mezzacapo, U. Las Heras, L. Lamata, E. Solano, S. Filipp, and A. Wallraff, *Phys. Rev. X* **5**, 021027 (2015).
- [52] M. Roth *et al.*, [arXiv:1808.04666](https://arxiv.org/abs/1808.04666).
- [53] D. Porras and J. I. Cirac, *Phys. Rev. Lett.* **92**, 207901 (2004).
- [54] R. Blatt and C. F. Roos, *Nat. Phys.* **8**, 277 (2012).
- [55] I. Arrazola, J. S. Pedernales, L. Lamata, and E. Solano, *Sci. Rep.* **6**, 30534 (2016).
- [56] O. V. Marchukov, A. G. Volosniev, M. Valiente, D. Petrosyan, and N. T. Zinner, *Nat. Commun.* **7**, 13070 (2016); A. G. Volosniev, D. Petrosyan, M. Valiente, D. V. Fedorov, A. S. Jensen, and N. T. Zinner, *Phys. Rev. A* **91**, 023620 (2015).
- [57] S. Whitlock, A. W. Glaetzle, and P. Hannaford, *J. Phys. B: At., Mol. Opt. Phys.* **50**, 074001 (2017).
- [58] T. L. Nguyen, J. M. Raimond, C. Sayrin, R. Cortinas, T. Cantat-Moltrecht, F. Assemat, I. Dotsenko, S. Gleyzes, S. Haroche, G. Roux, T. Jolicoeur, and M. Brune, *Phys. Rev. X* **8**, 011032 (2018).
- [59] C. Noh and D. G. Angelakis, *Rep. Prog. Phys.* **80**, 016401 (2017).
- [60] Y. P. Shim, S. Oh, X. Hu, and M. Friesen, *Phys. Rev. Lett.* **106**, 180503 (2011).
- [61] R. Toskovic *et al.*, *Nat. Phys.* **12**, 656 (2016).
- [62] O. Breunig, M. Garst, A. Klümper, J. Rohrkamp, M. Turbull, and T. Lorenz, *Sci. Adv.* **3**, eaa03773 (2017).
- [63] S. C. Benjamin and S. Bose, *Phys. Rev. A* **70**, 032314 (2004).
- [64] A. Bayat and S. Bose, *Phys. Rev. A* **81**, 012304 (2010); L. Banchi, A. Bayat, P. Verrucchi, and S. Bose, *Phys. Rev. Lett.* **106**, 140501 (2011).
- [65] S. R. White, *Phys. Rev. B* **48**, 10345 (1993).
- [66] A. Kolezhuk, R. Roth, and U. Schollwöck, *Phys. Rev. Lett.* **77**, 5142 (1996); *Phys. Rev. B* **55**, 8928 (1997).
- [67] U. Schollwöck, *Rev. Mod. Phys.* **77**, 259 (2003); *Ann. Phys. (NY)* **326**, 96 (2011).
- [68] The sign of  $J$  can be changed by local rotations of angle  $\pi$  around the  $z$  axis at even (or odd) sites  $j$ .
- [69] These cases are linked by a global rotation of angle  $\pi$  around the  $x$  or  $y$  axis, which leaves the coupling unchanged.
- [70] W. Dür, G. Vidal, and J. I. Cirac, *Phys. Rev. A* **62**, 062314 (2000).
- [71] C. H. Bennett, D. P. DiVincenzo, J. A. Smolin, and W. K. Wootters, *Phys. Rev. A* **54**, 3824 (1996).
- [72] S. Hill and W. K. Wootters, *Phys. Rev. Lett.* **78**, 5022 (1997); W. K. Wootters, *ibid.* **80**, 2245 (1998).
- [73] G. Vidal, *J. Mod. Opt.* **47**, 355 (2000).
- [74] V. Coffman, J. Kundu, and W. K. Wootters, *Phys. Rev. A* **61**, 052306 (2000).
- [75] T. J. Osborne and F. Verstraete, *Phys. Rev. Lett.* **96**, 220503 (2006).
- [76] We usually perform 20 sweeps keeping up to 900 states.

- [77] In a pure state with definite total magnetization  $M$  along  $z$ , the single-spin-reduced state  $\rho_i$  commutes with  $S_i^z \forall s$ . For  $s = \frac{1}{2}$  its eigenvalues are then  $\frac{1}{2} \pm \langle S_i^z \rangle$ , and its purity  $\text{Tr} \rho_i^2 = \frac{1}{2} + 2\langle S_i^z \rangle^2$ .
- [78] A. Böttcher and S. M. Grudsky, *Spectral Properties of Banded Toeplitz Matrices* (SIAM, Philadelphia, 2005).
- [79] G. Vidal and R. F. Werner, *Phys. Rev. A* **65**, 032314 (2002); K. Zyczkowski, P. Horodecki, A. Sanpera, and M. Lewenstein, *ibid.* **58**, 883 (1998).
- [80] A. Peres, *Phys. Rev. Lett.* **77**, 1413 (1996); M. Horodecki, P. Horodecki, and R. Horodecki, *Phys. Lett. A* **223**, 1 (1996).
- [81] J. H. H. Perk, H. W. Capel, M. J. Zuilhof, and Th. J. Siskens, *Phys. A (Amsterdam)* **81**, 319 (1975).
- [82] K. Okamoto and K. Yasumura, *J. Phys. Soc. Jpn.* **59**, 993 (1990).
- [83] N. Canosa and R. Rossignoli, *Phys. Rev. A* **75**, 032350 (2007).
- [84] S. Deng, G. Ortiz, and L. Viola, *Europhys. Lett.* **84**, 67008 (2008).
- [85] U. Divakaran, A. Dutta, and D. Sen, *Phys. Rev. B* **78**, 144301 (2008).
- [86] A. De Pasquale and P. Facchi, *Phys. Rev. A* **80**, 032102 (2009).
- [87] A. Dutta, G. Aeppli, B. K. Chakrabarti, U. Divakaran, T. F. Rosenbaum, and D. Sen, *Quantum Phase Transitions in Transverse Field Spin Models: From Statistical Physics to Quantum Information* (Cambridge University Press, Cambridge, UK, 2015).